IOPscience iopscience.iop.org

Home Search Collections Journals About Contact us My IOPscience

Spin density in Gd studied by magnetic Compton scattering

This article has been downloaded from IOPscience. Please scroll down to see the full text article.

1998 J. Phys.: Condens. Matter 10 10391

(http://iopscience.iop.org/0953-8984/10/46/006)

View the table of contents for this issue, or go to the journal homepage for more

Download details:
IP Address: 171.66.16.151
The article was downloaded on 12/05/2010 at 23:31

Please note that terms and conditions apply.

J. Phys.: Condens. Matter **10** (1998) 10391–10398. Printed in the UK PII: S0953-8984(98)97349-0

Spin density in Gd studied by magnetic Compton scattering

J A Duffy†, J E McCarthy†‡, S B Dugdale§, V Honkimäki‡, M J Cooper†, M A Alam‖, T Jarlborg§ and S B Palmer†

† Department of Physics, University of Warwick, Coventry CV4 7AL, UK
‡ ESRF, BP220, F-38043 Grenoble Cédex, France
§ Département de Physique de la Matière Condensée, Université de Genève, 24 quai Ernest Ansermet, CH-1211 Genève 4, Switzerland
‖ H H Wills Physics Laboratory, University of Bristol, Tyndall Avenue, Bristol BS8 1TL, UK

Received 30 April 1998

Abstract. The spin-dependent momentum density of single-crystal ferromagnetic gadolinium was probed by the magnetic Compton profile technique. Comparison with electronic structure calculations indicate that the local spin-density approximation is adequate for describing the magnetic Compton profiles. Furthermore, the linear combination of muffin-tin orbitals prescription compared favourably with a full-potential method. We find that testing theory against the experimental density of states is problematic. Our calculations also indicate that the spin density is sensitive to the treatment of the 5p electrons.

1. Introduction

Compared to the exotic magnetic structures that its neighbours exhibit, the magnetic order in Gd is relatively simple; below its Curie temperature of 294 K, the magnetic moment lies parallel to the *c*-axis, and remains so down to 232 K. At lower temperature the moment moves away from the *c*-axis, achieving a maximum deviation of about 65° at about 180 K [1], with the moments canted in a random cone structure. In contrast to the case for the ferromagnetic transition metals, its magnetism is thought to originate predominantly in the exchange field of the localized 4f electrons, rather than that of the conduction electrons [1].

The validity of local spin-density approximation (LSDA) calculations for 4f systems, and for Gd in particular, has been the subject of considerable discussion [2–6]. By treating the exchange and correlation as for a free-electron gas, the LSDA has produced poor agreement with experiment [7], due to the overestimation of the itineracy of the 4f electrons. Furthermore, there have been suggestions that the LSDA may be less reliable in magnetic, as compared with non-magnetic, systems; the LSDA underestimates the magnetic energy [8].

A magnetic Compton profile (MCP) is a one-dimensional projection of the momentum-space spin density, and, as such, can provide a sensitive test of band-structure calculations. Recent measurements on nickel using the MCP technique [9] showed discrepancies with LSDA and GGA (generalized gradient approximation) calculations performed using the combination of linear muffin-tin orbitals (LMTO) technique, and demonstrated the value of using a full-potential calculation. Because of the evident utility of the experimental technique, and the interest in gaining further understanding of the electronic structure of 4f systems, we present a study of ferromagnetic gadolinium. The method is described more fully in [10–12].

0953-8984/98/4610391+08$19.50 © 1998 IOP Publishing Ltd

Four measurements of the momentum-space spin density in Gd have been published previously; these were three magnetic Compton measurements [13–15] and one using positron annihilation [16]. However, the current results are the first at a temperature where the moment is parallel to the *c*-axis. Furthermore, they are the first to be able to offer the vital combination of high statistical precision and sufficiently good momentum resolution (an improvement of nearly a factor of two) for useful comparison with electronic structure calculations, and to provide some insight into the adequacy of the LSDA, and of the LMTO technique, for f-electron systems. For this study, we have performed the first LMTO calculations of the momentum-space spin density of Gd, within both the LSDA and the GGA.

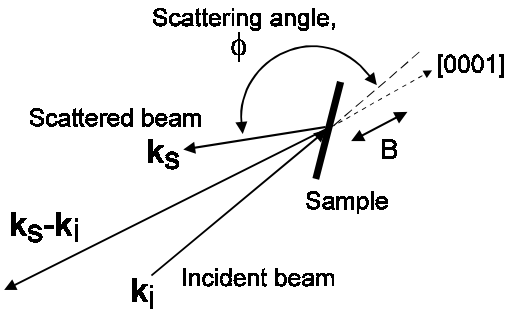

Figure 1. A schematic diagram depicting the scattering geometry adopted in this experiment. The magnetic field, $\boldsymbol{B}$, and hence also the spin moment, are reversed by rotating a 0.96 T permanent magnet. The *c*-axis was at 45° to the sample's surface.

2. Magnetic Compton scattering

In magnetic Compton scattering, the interest is in those electrons which are unpaired, and therefore contribute to the spin moment. If a spin moment exists, then this will be given by the difference in occupancy of the spin-up ($n\uparrow$) and spin-down ($n\downarrow$) bands:

$$\mu_{\text{spin}} = n\uparrow - n\downarrow. \tag{1}$$

This difference can be measured in a magnetic Compton experiment owing to the spin-dependent terms in the scattering cross-section. There have been numerous derivations of this inelastic scattering cross-section (see [10, 17], for example) which lead to the same general form, independently of whether free or bound electrons are considered. Here, we follow the cross-section in [18], taking a typical scattering geometry as depicted schematically in figure 1.

A reversible magnetic field, applied to the sample, is used to align its magnetic moment alternately parallel and antiparallel to the vector $\boldsymbol{k}_i \cos\phi + \boldsymbol{k}_s$. Here, $\boldsymbol{k}_i$ and $\boldsymbol{k}_s$ are the wave vectors of the incident and scattered beams, respectively, and ϕ is the scattering angle. This field flipping reverses the sign of the magnetic scattering contribution to the scattering cross-section, whilst leaving the charge scattering component unaltered. Thus, on subtracting two spectra, measured for two field directions, the charge contribution cancels, leaving only the magnetic term. This spin-dependent term leads directly to $J_{\text{mag}}(p_z)$, the twice-integrated spin-dependent momentum density, known as the magnetic Compton profile, or MCP, where

$$J_{\text{mag}}(p_z) = \int\int (n\uparrow(\boldsymbol{p}) - n\downarrow(\boldsymbol{p}))\ \mathrm{d}p_x\ \mathrm{d}p_y. \tag{2}$$

Here, $n\uparrow(\boldsymbol{p})$ and $n\downarrow(\boldsymbol{p})$ are the momentum-dependent spin densities. The area under the MCP is equal to the total spin moment per Wigner–Seitz cell:

$$\int_{-\infty}^{\infty} J_{\mathrm{mag}}(p_z)\ \mathrm{d}p_z = \mu_{\mathrm{spin}}. \tag{3}$$

Magnetic Compton scattering now represents an established technique for probing momentum-space spin densities and band structures in magnetic materials [10, 11]. Spin-polarized positron angular correlation experiments also probe the spin density [16, 19], but are subject to both positron–electron correlation effects, and repulsion of the positron by the positive-ion cores, so the positron does not sample electrons in all states equally [20]. The value of magnetic Compton scattering lies in its uniform sensitivity to the whole of the electron momentum distribution. The method is only sensitive to *spin* magnetic moments [10, 17, 21], within the impulse approximation [22]; that is to say, the orbital moment is not measured. One particular strength of the technique is that since the MCP is a difference between Compton profiles, the contributions from the non-magnetic electrons, and from unwanted systematic sources disappear.

3. Experimental details

The MCP for Gd was measured on the high-energy x-ray beamline (ID15) at the ESRF. The experiment was performed in a reflection geometry, as depicted in figure 1, with an incident beam energy of 200 keV, from a {311} reflection of the Si monochromator, and a scattering angle, ϕ, of 168°. The sample, a 5 mm diameter × 1.3 mm thick disk, was oriented such that the resolved direction was within ±2° of [0001]. The temperature of the sample was 235 ± 2 K, such that the sample's moment was still parallel to the experimentally resolved *c*-axis. The sample was magnetized alternately parallel and antiparallel to within ±1° of the resolved direction with a 0.96 T rotating permanent magnet. The energy distribution of the scattered x-rays was measured by a solid-state Ge detector. The momentum resolution obtained, of 0.44 atomic units (au, where 1 au $= 1.99 \times 10^{-24}$ kg m s^{-2}), was nearly a factor of two better than has been previously achieved for a Gd measurement [15]. The total number of counts (accumulated over 24 hours) in each of the charge profiles was 1.5×10^8, resulting in 3.7×10^6 in the MCP with a statistical precision of ±3% at the (magnetic) Compton peak in a bin of width 0.09 au. Following the usual correction procedures for the energy dependence of the detector efficiency, absorption, the relativistic scattering cross-section, and magnetic multiple-scattering [23], and after checking that the profiles were symmetric about zero momentum, the MCP was folded about this point, to increase the effective statistical precision of the data.

4. Electronic structure calculations

The spin-dependent momentum density was calculated within both the LSDA and GGA, using the prescriptions of Gunnarsson and Lunqvist [24] and Perdew and Wang [25], respectively. Detailed descriptions of the procedure can be found in [26]. Gd has an electron configuration $[\mathrm{Xe}]4f^{7}5d^{1}6s^{2}$, and, in the calculation, the 4f electrons were treated as valence states despite their core-like nature. If the 4f electrons were treated as core states, then there would be no hybridization between the s–d conduction band and the 4f minority band, contrary to expectation, which would affect the electronic structure significantly.

First, the electronic structure was calculated using the linearized muffin-tin orbital (LMTO) scheme [27, 28] at 252 points in the irreducible (1/24) wedge of the hexagonal

Brillouin zone, with a basis set of s, p, d and f functions. The core wavefunctions were treated fully relativistically, with all spin–orbit interactions considered; there was no spin–orbit coupling in the treatment of the valence electrons. This is reasonable, for in Gd there is no orbital contribution to the moment. After we had obtained a self-consistent potential, the valence electron wavefunctions were computed at 600 k-points in 1/8 of the Brillouin zone, in order to facilitate the calculation of the momentum distribution. The lattice parameter and c/a ratio were set to the experimental values of 0.3636 nm and 1.59 respectively. A second calculation then was performed, treating the 4f electrons as core states, and the resulting charge distribution was compared with that from a 'free-atom' calculation and that with the 4f electrons as valence states. It was found that these were all identical, indicating that the 4f states in the metal are as localized as in the free atom. This implies that the momentum distribution for the 4f electrons will have the same shape, whether the electrons are treated as valence or core. Owing to the limitation on the number of reciprocal-lattice vectors in the so-called 'overlap corrections' [26], the contribution of the 4f electrons was suppressed in the valence momentum density calculation and the 4f momentum distribution was calculated from the core states. The 4f and valence momentum distributions were then added in the case of the majority-spin channel. The momentum distribution of the majority spins was therefore a combination of the core 4f and the valence distributions, but with the wavefunctions still containing all of the necessary hybridization features. The momentum density was computed using 15 783 reciprocal-lattice vectors (extending to 11.5 au), with overlap corrections up to 3993 vectors. This was then projected onto [0001] to give the Compton profile, from which the MCP could be obtained. Following Temmerman and Sterne [2], we tried treating the semi-core 5p states as valence, and while the resulting bands did show some dispersion, the resulting MCP differed markedly from the experimental data. Hence, for the results presented here, the 5p states were treated as being in the core.

For comparison, we also show the results of a full-potential linearized augmented-plane-wave (FLAPW) calculation by Kubo and Asano [29], who treated exchange and correlation within the LSDA. The calculational details differed slightly, in that the ideal c/a ratio was used, along with a lattice constant of 0.3536 nm, rather than the experimental values. In their calculation of the Compton profile, 15 661 reciprocal-lattice vectors were included.

Table 1. Partial Gd charges for majority (↑) and minority (↓) electrons within the LSDA and GGA.

Potential	s	p	d	f	Total
LSDA ↑	0.401	0.339	1.100	6.986	8.826
LSDA ↓	0.371	0.163	0.521	0.119	1.174
GGA ↑	0.397	0.332	1.043	6.988	8.760
GGA ↓	0.372	0.180	0.576	0.112	1.240

The results of the calculations are presented in figure 2. The profile can be interpreted simply in terms of two separate contributions, namely that from the occupied 4f majority band (the broad component), and that originating in the spin polarization of the s–d conduction band. The chain line represents the Compton profile for the 4f electrons of a free atom of Gd, and is normalized to contain seven electrons. The three electronic structure calculations clearly show the extra contribution arising from the moment induced on the s–d electrons. The differences between these curves indicate the different moments predicted by the calculations.

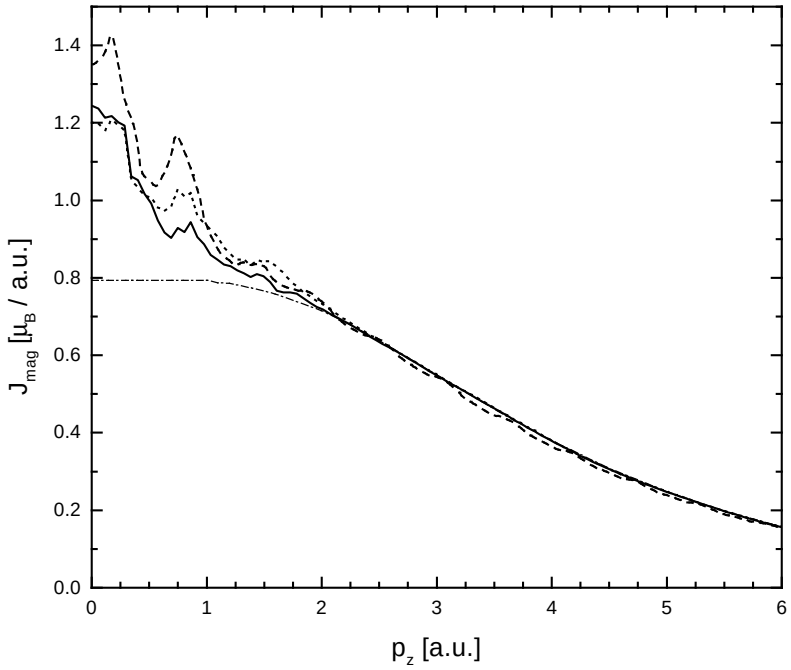

Figure 2. Calculations of the magnetic Compton profile of Gd [0001], using the LMTO-GGA (solid line), LMTO-LSDA (dotted line), and FLAPW-LSDA (dashed line). Also shown is the equivalent free-atom profile for Gd 4f, normalized to seven electrons.

5. Results and discussion

Before discussing the MCP results, it is instructive to examine the other ground-state properties derived from the calculations. From table 1, it can be seen that, as expected, most of the moment originates in the seven unpaired 4f electrons. The 4f bands showed almost no dispersion, reflecting their core-like nature. The spin moment in the LSDA and GGA were 7.65 μ_B and 7.52 μ_B respectively, compared with 7.70(8) μ_B from FLAPW-LSDA [29] and an experimental magnitude of 7.62 ± 0.01 μ_B [30]. These values were all obtained at low temperature; the calculations were effectively performed at $T = 0$ K, and the experimental data were measured at 4.2 K. Table 1 also shows that there is a moment, of mostly d character, associated with the conduction electrons, since the bands have been split by the 4f exchange field. The principal difference between the LSDA and GGA results is an overall reduction in the conduction electron polarization, particularly in the d contribution. In the current calculation, using the GGA does not improve the value of the predicted spin moment.

As in previous calculations, the density of states (DOS) at the Fermi level, $N(E_F)$, was much higher than the experimental value [31] of 21.35 states Ryd^{-1}/atom. The LDA and GGA calculations gave 29.27 and 31.01 states Ryd^{-1}/atom respectively. However, since the Fermi level lies on a steeply sloped part of the DOS, it is to be expected (and indeed it was found) that the DOS at E_F is extremely sensitive to the calculational parameters. The fact that LSDA calculations give a much higher DOS was explained by Bylander and Kleinman [4], as being due to the completely unoccupied minority 4f band appearing too close to the Fermi level, and the consequent strong hybridization of the s–d conduction bands with it.

The authors suggested that this was an artefact of the LSDA, arising because the localized 4f electrons were certainly not able to play a role in screening any valence–valence exchange interactions. In a subsequent article [5], they proceeded to show that a DOS closer to the experimental value was obtained by modifying the potential so that the conduction electrons felt an LSDA potential from each other and a Hartree–Fock potential from the core electrons. This *ad hoc* procedure involved parametrizing the exchange functional to give the 'correct' magnetization. However, the LMTO calculations show that, owing to the position of the Fermi energy on a peaked part of the DOS (as a consequence of the minority f bands lying just above E_F), it is possible to induce large changes in the DOS by making relatively small changes in the linearization energies. Hence, agreement with the experimental DOS at E_F is not necessarily a good test of the theory.

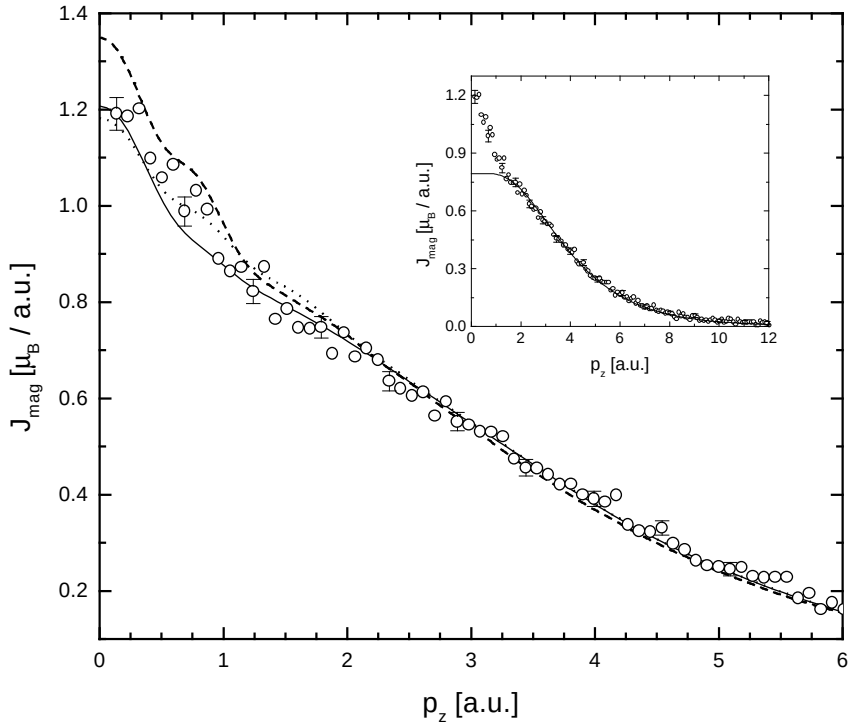

Figure 3. The experimental magnetic Compton profile of Gd, normalized to 7.62 μ_B (open circles) together with the calculations presented in figure 2. Here, the theoretical profiles have been convoluted with a Gaussian with FWHM = 0.44 au to represent the experimental resolution. The inset shows the extent of the 4f contribution to the experimental MCP, together with the relativistic Hartree–Fock free-atom 4f profile (solid line).

The experimental magnetic Compton profile is presented in figure 3, together with the theoretical predictions, convoluted with the (Gaussian) experimental resolution function with width 0.44 au. The profiles are normalized to their respective predicted moments, and the experimental data are normalized to the known value of 7.62 μ_B. As in the previous MCP measurements of Brahmia *et al* [14] and Sakai *et al* [15], these measurements show the s–d conduction electron contribution superposed on that from the 4f. The pioneering positron measurement [16] showed almost no evidence of the 4f component; in such systems a positron annihilates preferentially with the itinerant s–d electrons, since the overlap of its

wavefunction with those of the deep-lying 4f states is very small.

In the high-momentum tails the agreement between the relativistic Hartree–Fock free-atom 4f Compton profile [32] and the data is excellent. This is expected from energy considerations [11]. In addition to this, as one would anticipate for such a localized state (there is almost no dispersion in the band), the 4f contribution predicted in the LMTO calculations also agrees well. In contrast with the case for Ni [9], this agreement extends to lower momenta, with discrepancies only apparent below $p_z = 2$ au.

In the low-momentum region, the induced s–d spin moment contributes to the MCP, and solid-state effects are observed. Here, the theoretical work exhibits discrepancies when compared to the experimental data. In contrast to Ni, where the FLAPW method outperforms LMTO, here the use of a full potential appears to confer no advantage. Indeed, in terms of the size of the induced moment, the LMTO technique is better, with the LSDA result closest to the expected value. This is reflected in the MCP: at $p_z = 0$ au both LMTO predictions agree well with experiment, whereas the FLAPW method overestimates the spin density. The performance of the LMTO calculations is much better than that observed for the 3d ferromagnets. As for the MCPs in ferromagnetic nickel [9], it is difficult to choose one approximation as preferable.

6. Conclusions

The spin density of Gd in momentum space was measured using the magnetic Compton profile technique. Calculations of the spin density, using the FLAPW and LMTO methods, compared favourably with the experimental results. Invoking the GGA does not produce any notable improvement in the profile shape. In contrast with the case for nickel, where a full-potential calculation produced a significant improvement, the LMTO calculation works just as well.

The experiment showed that high-quality data can be obtained using the magnetic Compton scattering technique. The good agreement between theory and experiment implies that employing the combined LSDA and Hartree–Fock procedure adopted by Bylander and Kleinman [5] is not necessary. Furthermore, we conclude that testing theory against the experimental DOS is problematic; its predicted value is strongly dependent on the calculational parameters. Our calculations indicate that the spin density is sensitive to the treatment of the 5p electrons. Further calculations will be performed to investigate the significance of this relationship in detail.

The ability of the LMTO technique to describe the spin density of Gd, and in particular the induced s–d spin moment, is of significance because it may now be used confidently to predict the behaviour of Gd alloys. For example, there is much interest in the magnetic properties of the Gd–Y system [33, 34], which are driven by the electronic structure. This system will be the subject of a forthcoming publication by the current authors.

Acknowledgments

We would like to thank the ESRF for the allocation of beam time, and the EPSRC (UK) for generous financial support. One of us (SBD) would like to thank the Royal Society (UK) and the Swiss National Science Foundation for a Fellowship. The authors would also like to thank Professor Y Kubo for making his FLAPW data available.

References

[1] Cracknell A P and Wong K C 1973 *The Fermi Surface* (Oxford: Oxford University Press)
[2] Temmerman W M and Sterne P A 1990 *J. Phys.: Condens. Matter* **2** 5529
[3] Singh D J 1994 *Phys. Rev.* B **44** 7451
[4] Bylander D M and Kleinman L 1994 *Phys. Rev.* B **49** 1608
[5] Bylander D M and Kleinman L 1994 *Phys. Rev.* B **50** 1363
[6] Heinemann M and Temmerman W M 1994 *Phys. Rev.* B **49** 4348
[7] Min B I, Jansen H J F, Oguchi T and Freeman A J 1986 *J. Magn. Magn. Mater.* **59** 277
[8] Wang C S, Klein B M and Krakauer H 1985 *Phys. Rev. Lett.* **54** 1852
[9] Dixon M A G, Duffy J A, Gardelis S, McCarthy J E, Cooper M J, Dugdale S B, Jarlborg T and Timms D N 1998 *J. Phys.: Condens. Matter* **10** 2759
[10] Sakai N 1996 *J. Appl. Crystallogr.* **29** 81
[11] Cooper M J 1997 *J. Radiat. Phys. Chem.* **50** 63
[12] Lovesey S W and Collins S P 1996 *X-ray Scattering and Absorption by Magnetic Materials* (Oxford: Clarendon)
[13] Mills D M 1987 *Phys. Rev.* B **36** 6178
[14] Brahmia A, Cooper M J, Timms D N, Collins S P, Kane P P and Laundy D 1989 *J. Phys.: Condens. Matter* **1** 3879
[15] Sakai N, Tanaka Y, Itoh F, Sakurai H, Ito M, Kawata H and Iwazumi T 1991 *J. Phys. Soc. Japan. Lett.* **60** 1201
[16] Hohenemser C, Weingart J M and Berko S 1968 *Phys. Lett.* **28A** 41
[17] Lovesey S W 1996 *J. Phys.: Condens. Matter* **8** L353
[18] McCarthy J E, Cooper M J, Honkimäki V, Tschentscher T, Suortti P, Gardelis S, Hämäläinen K, Manninen S O and Timms D N 1997 *Nucl. Instrum. Methods* **401** 463
[19] Genoud P, Manuel A A, Walker E and Peter M 1991 *J. Phys.: Condens. Matter* **3** 4201
[20] West R N 1995 *Proc. Int. Enrico Fermi School of Physics: Positron Spectroscopy of Solids* ed A Dupasquier and A P Mills Jr (Amsterdam: IOS)
[21] Cooper M J, Zukowski E, Collins S P, Timms D N, Itoh F and Sakurai H 1992 *J. Phys.: Condens. Matter* **4** L399
[22] Carra P, Fabrizio M, Santoro G and Thole B T 1996 *Phys. Rev.* B **53** R5994
[23] Bell F, Felsteiner J and Pitaevskii L P 1996 *Phys. Rev.* A **53** R1213
[24] Gunnarsson O and Lunqvist B I 1976 *Phys. Rev.* B **13** 4274
[25] Perdew J P 1985 *Phys. Rev. Lett.* **55** 1665
Perdew J P and Wang Y 1986 *Phys. Rev.* B **33** 8800
Perdew J P 1986 *Phys. Rev.* B **33** 8822
Perdew J P 1986 *Phys. Rev.* B **34** 746
[26] Jarlborg T and Singh A K 1985 *J. Phys. F: Met. Phys.* **15** 727
[27] Andersen O K 1975 *Phys. Rev.* B **12** 3060
Jarlborg T and Arbman G 1977 *J. Phys. F: Met. Phys.* **7** 1635
[28] Barbiellini B, Moroni E G and Jarlborg T 1990 *J. Phys.: Condens. Matter* **2** 7597
[29] Kubo Y and Asano S 1992 *J. Magn. Magn. Mater.* **115** 177
[30] Roeland L W, Cock G J, Mueller F A, Moleman A C, McKewen K A, Jordan R G and Jones D W 1975 *J. Phys. F: Met. Phys.* **5** L233
[31] Wells P, Lanchester P C, Jones D W and Jordan R G 1974 *J. Phys. F: Met. Phys.* **4** 1729
[32] Biggs F, Mendelsohn L B and Mann J B 1975 *At. Data Nucl. Data Tables* **16** 201
[33] Bates S, Palmer S B, Sousa J B, McIntyre G J, Fort D, Levgold S, Beaudry B J and Koehler W C 1985 *Phys. Rev. Lett.* **55** 2968
[34] Foldeaki M, Chahine R and Bose T K 1995 *Phys. Rev.* B **52** 3471